JACS
JOURNAL OF THE AMERICAN CHEMICAL SOCIETY
Article
pubs.acs.org/JACS

High-Throughput Enantiopurity Analysis Using Enantiomeric DNA-Based Sensors

Trevor A. Feagin, David P. V. Olsen, Zachary C. Headman, and Jennifer M. Heemstra*

Department of Chemistry and the Center for Cell and Genome Science, University of Utah, Salt Lake City, Utah 84112, United States

Supporting Information

ABSTRACT: Distinguishing between the two enantiomers of a molecule is a challenging task due to their nearly identical physical properties. Time-consuming chromatography methods are typically required for this task, which greatly limits the throughput of analysis. Here we describe a fluorescence-based method for the rapid and high-throughput analysis of both small-molecule enantiopurity and concentration. Our approach relies on selective molecular recognition of one enantiomer of the target molecule using a DNA aptamer, and the ability of aptamer-based biosensors to transduce the presence of a target molecule into a dose-dependent fluorescence signal. The key novel aspect of our approach is the implementation of enantiomeric DNA biosensors, which are synthesized from D- and L-DNA, but labeled with orthogonal fluorophores. According to the principle of reciprocal chiral substrate specificity, these biosensors will bind to opposite enantiomers of the target with equal affinity and selectivity, enabling simultaneous quantification of both enantiomers of the target. Using the previously reported DNA biosensor for L-tyrosinamide (L-Tym), we demonstrate the ability to rapidly and accurately measure both enantiopurity and concentration for mixtures of L- and D-Tym. We also apply our enantiomeric biosensors to the optimization of reaction conditions for the synthesis of D-Tym and provide mathematical modeling to suggest that DNA biosensors having only modest binding selectivity can also be used for fluorescence-based enantiopurity measurement. This research provides a generalizable method for high-throughput analysis of reaction mixtures, which is anticipated to significantly accelerate reaction optimization for the synthesis of high-value chiral small molecules.

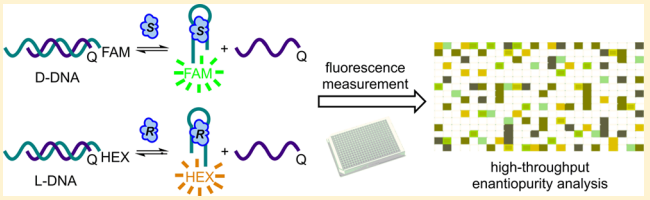

INTRODUCTION

Biological systems are exquisitely adept at producing small organic molecules with high stereoselectivity, as different stereoisomers of a molecule can illicit markedly different biological effects.[1] Achieving high stereoselectivity plays an equally important role in many applications of synthetic organic chemistry, as the target molecules are often intended to interact with biological systems, for example in the case of small-molecule therapeutics. Asymmetric catalysis has proven to be a revolutionary technology for the stereoselective synthesis of small molecules,[2] and high-throughput screening (HTS) can be used to accelerate the optimization of reaction conditions for a particular synthetic transformation.[3−10] In HTS, reaction conditions including catalyst, solvent, and temperature can be sampled combinatorially, and the implementation of robotics enables a large number of reactions to be run in parallel. However, the analysis of these reaction mixtures for yield and stereoselectivity remains a severe bottleneck that hinders the discovery of improved catalysts and reaction conditions.

Chemical reactions that produce a mixture of enantiomers pose an especially challenging analysis problem, as enantiomers have nearly identical physical properties. The current gold standard for measuring yield and enantiopurity is chiral high performance liquid chromatography (HPLC). However, even under optimized conditions, HPLC is only capable of analyzing approximately 800 samples per day.[11,12] A large number of alternative analysis platforms have been explored, including gas chromatography (GC),[13] capillary electrophoresis (CE),[14−16] circular dichroism (CD),[17−19] infrared thermography,[20] mass spectrometry (MS),[21,22] and enzymatic methods.[23] Notably, new MS methods have been developed that enable the analysis of up to 10 000 samples per day,[22] but even this level of throughput is not sufficient to scan the vast libraries of reaction mixtures that can plausibly be generated in catalyst development and reaction optimization.[3] Moreover, many of these methods can accurately analyze enantiopurity, but provide little information regarding reaction yield.

In contrast to the analysis platforms listed above, fluorescence-based methods have potential to enable exceptionally high throughput, as a 1536-well plate can be analyzed in less than 1 min.[24] A number of laboratories have reported elegant approaches for fluorescence-based enantiopurity analysis of small molecules containing specific functional groups, such as α-hydroxycarboxylates, diols, and carboxylic acids.[25−27] We envisioned the development of a complementary approach in which a single small-molecule target (or small handful of structurally similar targets) can be rapidly analyzed

Received: January 27, 2015
Published: March 6, 2015

DOI: 10.1021/jacs.5b00923
J. Am. Chem. Soc. 2015, 137, 4198−4206

for enantiopurity, but without the requirement for specific functional groups. While this approach may find limitations for use in the development of new reaction methodologies, where large substrate scope is beneficial, it is ideal for use in reaction development for high-value compounds, such as pharmaceuticals and their synthetic intermediates. In the latter case, a tremendous amount of effort is focused on the development of optimized reaction conditions for a single molecule or small subset of molecules, and thus, achieving high throughput takes priority over substrate scope.

Our approach to high-throughput enantiopurity analysis relies on molecular recognition of the target molecule using a DNA aptamer. Aptamers are short nucleic acid sequences that can be generated in vitro to bind a wide range of targets including small molecules, proteins, and cell types.[28−30] Importantly, because aptamers are generated in vitro, negative selections can be utilized to increase substrate selectivity, and aptamers have been reported which bind to one enantiomer of a small molecule with greater than 10 000:1 selectivity over the opposite enantiomer.[31] In utilizing aptamers for high-throughput enantiopurity measurement, the first key element to our approach is the concept of reciprocal chiral substrate selectivity. DNA is a chiral molecule, and thus, if a native D-DNA aptamer binds selectively to one enantiomer of a small molecule, then by definition, the same aptamer sequence synthesized from non-native L-DNA (referred to as the Spiegelmer from the German word "Spiegel" meaning "mirror")[32−35] will bind to the opposite enantiomer of the small molecule with identical selectivity and affinity (Figure 1).

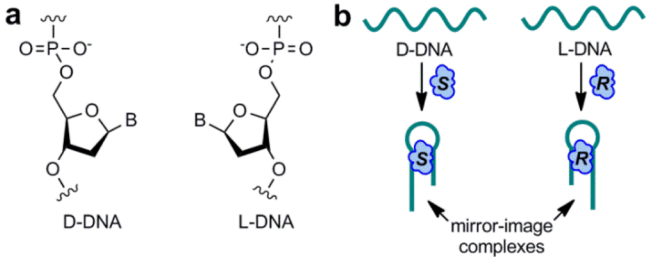

Figure 1. (a) Chemical structures of native D-DNA and enantiomeric L-DNA (Spiegelmer). (b) In accordance with the principle of reciprocal chiral substrate selectivity, D- and L-DNA aptamers will bind to opposite enantiomers of a small-molecule target with equal affinity and selectivity to give mirror-image complexes.

The second key element to our approach is the ability of nucleic acid aptamers to transduce the presence of a specific molecule into a dose-dependent fluorescence output. This can be achieved in a number of formats,[36] and for our enantiopurity analysis approach, we chose to utilize what is arguably the most straightforward of these formats, the structure-switching (SS) biosensor.[37,38] In the SS biosensor format, a short complementary strand is hybridized to the aptamer via Watson−Crick base pairing. However, in the presence of the target molecule, the aptamer preferentially binds to the target, displacing the complementary strand. If the aptamer and complementary strand are labeled with a fluorophore and quencher, respectively, then the target ligand will produce a dose-dependent increase in fluorescence signal.

Applying the concept of reciprocal chiral substrate selectivity to SS biosensors, we designed a system in which the D- and L-DNA biosensors are synthesized having orthogonal fluorophores (Figure 2a). These enantiomeric sensors can then be added together to a solution of the target molecule, and two-

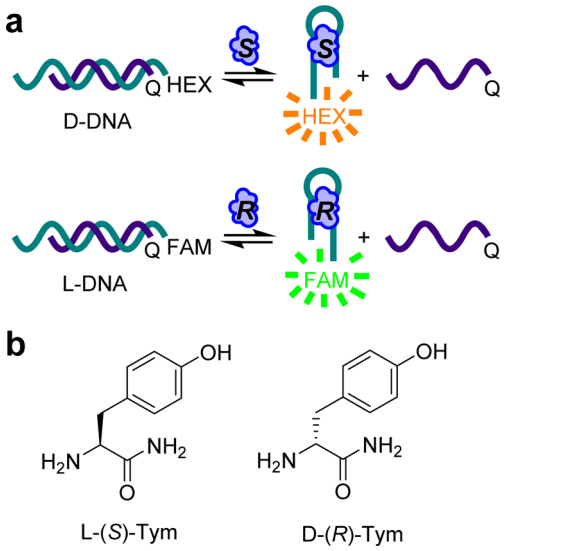

Figure 2. (a) Enantiomeric structure-switching biosensors are functionalized with orthogonal fluorophores, enabling simultaneous quantification of both enantiomers of the target molecule. HEX = hexachlorofluorescein; FAM = fluorescein. (b) Chemical structures of L- and D-Tym.

color fluorescence measurement used to provide the concentration of each enantiomer of the target, in turn providing both yield and enantiopurity. We note that upon addition of different fluorophores to the D- and L-DNA biosensors, these complexes are no longer perfect enantiomers. However, we find that this subtle difference in chemical structure has only a minor impact on the performance of the biosensors, and does not alter their ability to behave according to the principle of reciprocal chiral substrate selectivity. Thus, while the D- and L-DNA biosensors in our study are not true enantiomers, for simplicity we will refer to them as enantiomeric.

Using the previously reported SS biosensor for L-tyrosinamide (L-Tym, Figure 2b),[39] we demonstrate here the ability to rapidly and accurately measure both enantiopurity and concentration for mixtures of L- and D-Tym. To demonstrate the utility of this approach, we apply our enantiomeric biosensors to the optimization of reaction conditions for the synthesis of D-Tym. We demonstrate that our fluorescence-based approach not only allows rapid screening of multiple conditions and reaction time-points, but has potential to enable near real-time analysis. We also provide mathematical analysis to suggest that SS biosensors having only modest binding selectivity can also be used for fluorescence-based enantiopurity measurement. Together, this research provides a novel method for the high-throughput analysis of enantiopurity that can be adapted for use with a diverse array of small molecule targets and has potential to enable screening of ~10^5 to 10^6 reaction mixtures per day. Achieving this high level of throughput in a generalizable format is anticipated to significantly accelerate reaction optimization for the synthesis of high-value chiral small molecules.

MATERIALS AND METHODS

General. Unless otherwise noted, all starting materials were obtained from commercial suppliers and used without further

DOI: 10.1021/jacs.5b00923
J. Am. Chem. Soc. 2015, 137, 4198−4206

Table 1. Sequences of the Aptamer and Complementary Strands Tested during Biosensor Optimization[a]

Name	Sequence (5'-3')
aptamer	FAM/HEX-TGGAGCTTGGATTGATGTGGTGTGTGAGTGCGGTGCCC
CS-09	CACATCAAT-BHQ1
CS-10	CACATCAATC-BHQ1
CS-11	CACATCAATCC-BHQ1
CS-12	CACATCAATCCA-BHQ1

[a]The underlined region of the aptamer indicates the complementary strand binding site.

purification. All DNA was purchased from the University of Utah DNA/Peptide Synthesis Core Facility. All absorbance and fluorescence values were recorded using a Biotek Synergy Mx microplate reader.

Modifiers Used for DNA Synthesis. Fluorescein and hexachlorofluoroscein dyes were installed using phosphoramidites from Glen Research. Black Hole quencher 1 was installed using CPG cartridges from Glen Research. L-DNA was prepared using phosphoramidites from ChemGenes.

Preparation of Biosensor Stocks. Binding buffer (10 mM Tris-HCl, 100 mM NaCl, 5 mM KCl, 2 mM $MgCl_2$, 1 mM $CaCl_2$, pH 7.5) was used for all DNA stock solutions. DNA biosensors were prepared by generating a solution containing 1 μM aptamer and 2.5 μM complementary strand in binding buffer. This solution was incubated at 90 °C for 10 min, then rapidly cooled and stored at 4 °C. Prior to use, the solution was allowed to warm to room temperature.

Enantiopurity Measurement. A volume of 50 μL of a sample containing varying concentrations of L- and D-Tym was combined with 50 μL of the biosensor stock solution described above to give a 100 μL sample having concentrations of 500 nM aptamer and 1.25 μM complementary strand. These samples were then transferred to a Costar 96-well black flat bottom polystyrene plate. The plates were covered and incubated at 25 °C for 20 min and subsequently scanned for fluorescence intensity using excitation/emission wavelengths of 490/520 nm (FAM) and 524/572 nm (HEX). Fluorescence values were standardized using a control solution containing only fluorophore-labeled aptamer.

Reaction Progress. All reactions were carried out in 200 μL PCR tubes using a Bio-Rad PTC-1148 thermocycler for temperature control. D-Tyrosine ethyl ester was added to 100 μL of NH_4OH to a final concentration of 10 mM. Reactions were quenched by diluting the reaction mixture into of 9.9 mL of binding buffer containing the biosensors at specified time points. Samples were then analyzed as described above.

HPLC Validation. We were unable to achieve baseline separation of L- and D-Tym using a commercially available HPLC column. Thus, we developed the following method for purification, hydrolysis, and analysis of our reaction mixtures. Samples from the reaction carried out at 50 °C were lyophilized and desalted. The L/D-Tym was separated from the remaining unreacted Tyr-OEt by HPLC using 60:40 water:MeOH (Agilent ZORBAX Eclipse XDB-C18, 5 μm, 9.4 × 250 mm). Collected fractions were lyophilized and resuspended in 100 μL water. The solutions were then added to H-form Dowex and reacted for 24 h at 100 °C to hydrolyze the tyrosinamide to tyrosine. Dowex was removed using 0.2 μm centrifuge spin filters (Millipore UFC30GV00), and the L/D-Tyr was purified by HPLC using 60:40 water:MeOH (Agilent ZORBAX Eclipse XDB-C18, 5 μm, 9.4 × 250 mm). The Tyr fraction was then analyzed by chiral HPLC (Astec Chirobiotic T 25 cm × 4.6 mm) using 20:80 water:MeOH with 0.02% formic acid. Enantiomeric ratios were calculated by integration of peak areas and compared to those measured using the DNA biosensors.

RESULTS AND DISCUSSION

To demonstrate the utility of our enantiopurity analysis method, we utilized the previously reported DNA aptamer for L-Tym. This aptamer was first reported by Gatto and co-workers in 2001,[40] and in 2011, was elaborated into an SS biosensor by Peyrin and co-workers.[39] The SS biosensor developed by Peyrin was utilized for L-Tym detection by fluorescence polarization (FP), so the aptamer was unfunctionalized, and the complementary strand was labeled with a fluorophore. For our biosensing format, we instead functionalized the termini of the aptamer and complementary strand with a fluorophore and quencher, respectively, to enable small-molecule quantification using a standard fluorescence plate reader.

Identifying an Appropriate Fluorophore Pair. For our orthogonal fluorophores to be used on the D- and L-DNA aptamers, we initially chose fluorescein (FAM) and cyanine 3 (Cy3). However, initial results showed that the Cy3 biosensor had a K_{sens} value (defined as the ligand concentration at which half of the aptamer strands are dehybridized from their complementary strands) 2-fold higher than that of the FAM biosensor. Similar results demonstrating the differential impact of cationic and anionic dyes on aptamer-complementary strand binding have been reported by Peyrin and co-workers.[39] Therefore, in refining our enantiomeric dual biosensors, we sought to use dyes having similar chemical properties, as this was hypothesized to result in biosensors having similar K_{sens} values. We found that hexachlorofluorescein (HEX) and FAM were an ideal fluorophore pair for our dual biosensors, as these fluorophores have very similar electronic and structural properties, and have excitation/emission maxima of 524/572 nm (HEX) and 490/520 nm (FAM), making them spectrally orthogonal. Furthermore, Black Hole quencher 1 (BHQ1) effectively quenches both FAM and HEX, minimizing the difference in chemical modifications. To validate the orthogonality of our fluorescent biosensors, we carried out an experiment in which solutions were prepared having the D-DNA aptamer functionalized with HEX, the L-DNA aptamer functionalized with FAM, or an equal mixture of the two aptamers. All samples were analyzed for fluorescence intensity using excitation/emission wavelengths of 490/520 nm and 524/572 nm, and we observed significant signal above background for each biosensor using its target wavelengths, but no signal was detectible above background when using the off-target wavelengths (Supporting Information Figure S1). Thus, we decided to utilize HEX-BHQ1 and FAM-BHQ1 as our fluorophore−quencher pairs in all subsequent SS biosensors.

Biosensor Design and Optimization. Our first consideration in biosensor optimization was to screen buffer conditions for those that provided the highest selectivity and lowest fluorescence background. We used the conditions reported by Peyrin as a starting point for optimization, but found that for our assay, a higher ionic strength was beneficial.

DOI: 10.1021/jacs.5b00923
J. Am. Chem. Soc. 2015, 137, 4198−4206

This optimized binding buffer (10 mM Tris-HCl, 100 mM NaCl, 5 mM KCl, 2 mM $MgCl_2$, 1 mM $CaCl_2$, pH 7.5) was used for all of the following experiments.

It is well established that the length and binding position of the complementary strand can have a large impact on the hybridization and ligand binding characteristics of SS biosensors,[41] and a number of complementary strand sequences have previously been tested for use with the L-Tym aptamer in CE and FP experiments.[16,39] Upon the basis of these previous reports, we synthesized and tested four BHQ1-labeled complementary strands having various lengths (Table 1). Each of these complementary strands were incubated with HEX-labeled L-Tym (D-DNA) aptamer and increasing concentrations of L-Tym. After allowing 20 min for equilibration, the percent displacement (%D) for each biosensor was calculated using eq 1

$$\%D = \left(\frac{F - F_0}{F_m - F_0}\right) \times 100 \quad (1)$$

in which F is the measured fluorescence, F_0 is the fluorescence of the biosensor in the absence of ligand, and F_m is the fluorescence of the aptamer alone. We compared %D values for the different complementary strand sequences to determine which sequence provided the greatest signal-to-noise ratio across a wide range of ligand concentrations. Of those tested, we found that CS-09 showed the best signal-to-noise ratio at 25 °C (Figure 3).

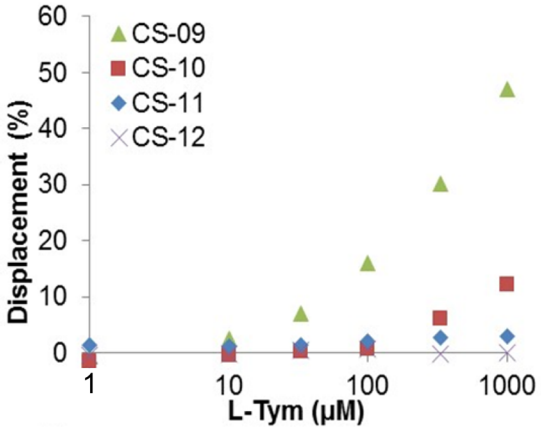

Figure 3. Complementary strand length strongly impacts the responsiveness of the SS biosensor. CS-09 was chosen for all subsequent enantiopurity analysis experiments.

The concentrations and stoichiometry of the aptamer and complementary strand can also have a dramatic impact on K_{sens}, as these factors influence the position of equilibrium for hybridization of the two DNA strands, which is in direct competition with the equilibrium of ligand binding. Therefore, to optimize aptamer and complementary strand concentrations and stoichiometry, we first prepared 6 solutions of the D-DNA biosensor having a 1:1 aptamer:complementary strand stoichiometry, but having concentrations of each strand varying from 30 nM to 1 μM. A binding isotherm for hybridization of the aptamer and complementary strand was produced by plotting the concentration versus percent displacement (Supporting Information Figure S2). At lower concentrations, high background fluorescence was observed, presumably because equilibrium favors dehybridization of the aptamer and complementary strand. However, calculations from our binding isotherm indicated that at 500 nM, approximately 90% of the aptamer strands were hybridized to a complementary strand. We reasoned that this approximate level of hybridization would be suitable for our enantiopurity assay, as the majority of biosensors are assembled, minimizing background and maximizing potential signal gain. However, the presence of a small number of disassembled biosensors suggests that the mixture is perched at an equilibrium where small perturbations in the energetics of the system (e.g., through the introduction of target ligand) are likely to produce large shifts in the ratio of assembled:disassembled biosensors, and thus fluorescence signal.

In addition to optimizing concentration, we also systematically investigated the effect of aptamer:complementary strand stoichiometry on signal-to-background ratio. Similar to overall concentration, varying the stoichiometry of the aptamer and complementary strand shifts the equilibrium for assembly of the biosensor, and thus impacts both background and signal gain. Five samples were prepared having 500 nM aptamer and a 1:1, 1:1.5, 1:2, 1:2.5, or 1:3 aptamer:complementary strand ratio. Each sample was tested with increasing L-Tym concentrations, and we found that the 1:2.5 ratio provided the greatest signal-to-noise ratio (Supporting Information Figure S3). Thus, we identified 500 nM aptamer and 1.25 μM complementary strand as the ideal concentrations for use in our enantiopurity assays.

Enantioselectivity and Specificity of Biosensors. Having optimized the sequences and concentrations of the SS biosensors, we next turned to analyzing target binding selectivity. First, the biosensors were individually tested for binding to L- and D-Tym. The data in Figure 4a,b illustrate that the biosensors bind to Tym with a high degree of enantioselectivity, as fluorescence signal was observed for the target enantiomer at concentrations as low as 3−10 μM, but no binding of the off-target enantiomer was detected up to 1 mM.

To test the effect of side chain structure on aptamer binding, glycinamide (Glm), racemic alaninamide (Alm), and both L- and D-phenylalaninamide (L-Phm and D-Phm) were incubated with the biosensors and fluorescence intensity measured (Figure 4c,d). Glm and Alm were chosen because they are the least-functionalized nonchiral and chiral amino amides, respectively. Thus, binding information for these molecules would reveal the role of the phenyl side chain and chiral center in aptamer recognition. No signal was observed for either of these targets at concentrations up to 1 mM, suggesting that the phenyl side chain is critical to aptamer binding. In contrast, L- and D-Phm were found to bind enantioselectively to the SS biosensors, showing a similar trend to L- and D-Tym, but with a weaker binding affinity. We interpret this result to indicate that the hydroxyl functionality of Tym likely interacts with the aptamer via a hydrogen bonding interaction, and that this interaction strengthens, but is not critical to, target binding. Finally, the importance of the amino amide functionality was investigated using L- and D-tyrosine ethyl ester (L-Tyr-OEt and D-Tyr-OEt). As selectivity for Tym over Tyr-OEt is necessary for the reaction monitoring experiments described below, we were pleased to observe no signal for L- or D-Tyr-OEt at concentrations up to 1 mM. Collectively, these data indicate that the chirality, phenyl side chain, and amide functionality all play critical roles in binding of the aptamer to the target, and the presence of a hydroxyl group on the phenyl ring enhances the strength of the aptamer−target binding interaction.

DOI: 10.1021/jacs.5b00923
J. Am. Chem. Soc. 2015, 137, 4198−4206

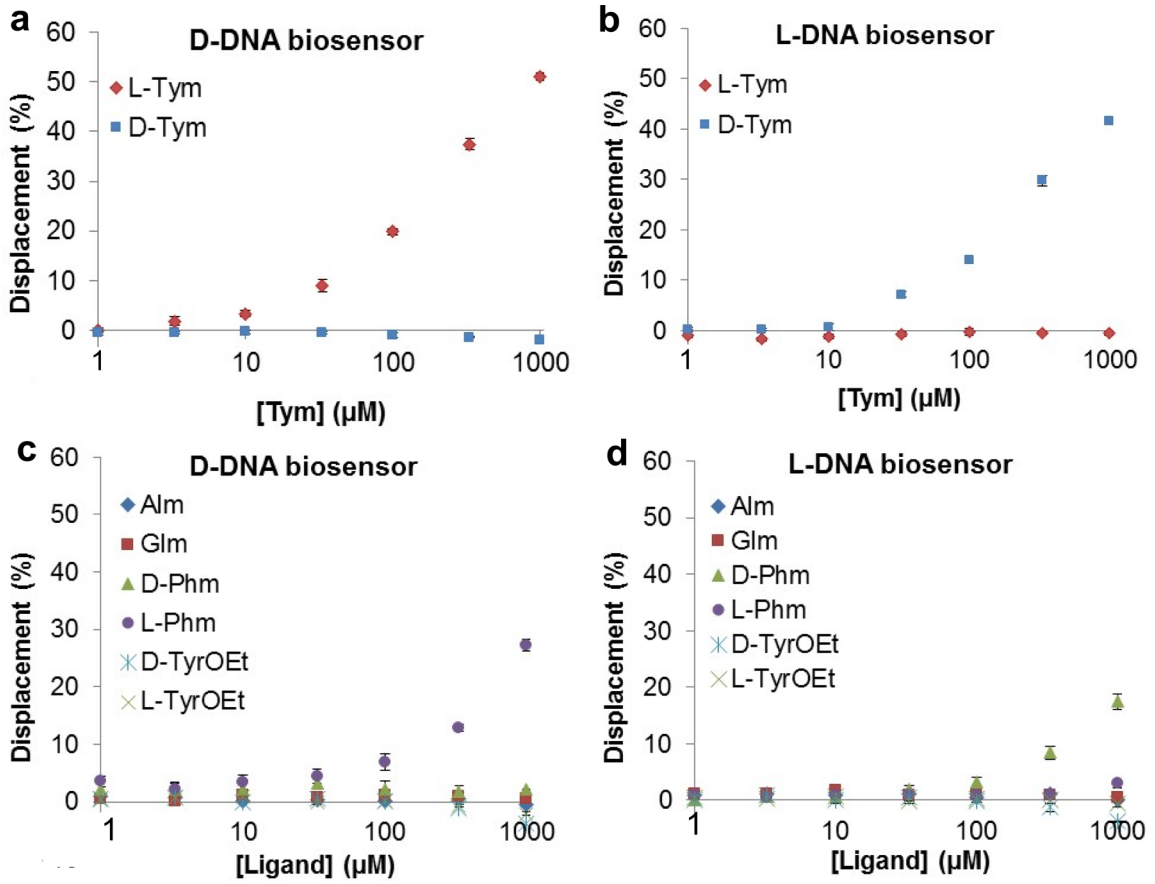

Figure 4. Fluorescence response of (a) D-DNA and (b) L-DNA biosensors to L- and D-Tym. Fluorescence response of (c) D-DNA and (d) L-DNA biosensors to structurally related compounds. All data represent an average of three trials.

In principle, enantiomeric D- and L-DNA biosensors should bind to opposite enantiomers of a given small-molecule target with identical K_{sens} values. However, the data in Figure 4 show that the L-DNA biosensor consistently gives slightly smaller % displacement values compared to the D-DNA biosensor. We hypothesize that this difference arises from the fact that our biosensors are not perfectly enantiomeric. The FAM and HEX fluorophores, while carefully selected, have different electronic properties, which can impact binding of the aptamer to the displacement strand, leading to differences in target-dependent displacement. However, it is important to note that we use calibration curves as described below to solve for the concentration of each enantiomer. Thus, these subtle differences in biosensor response will not impact the accuracy of our enantiopurity measurements.

Enantiopurity Analysis for Mixtures of L- and D-Tym. As seen in Figure 4a,b, the fluorescence response of the SS biosensors follows a Langmuir isotherm. This is to be expected, as the fluorescence signal results from an equilibrium binding interaction between the aptamer and the target. Thus, we reasoned that by maintaining substrate concentrations below saturation, we could construct calibration curves to enable quantitative analysis of unknown samples. Importantly, the use of % displacement instead of raw fluorescence intensity enables the calibration curve to be applied across samples analyzed on different days and potentially on different pieces of instrumentation.

To construct the calibration curves, the L- and D-DNA biosensors were combined together in a single solution and incubated with varying concentrations of L- and D-Tym. In each solution, the total Tym concentration was held at constant at 500 μM, and the D:L ratio of the Tym was systematically varied from 100:0 to 0:100. Each solution was analyzed using excitation/emission wavelengths of 490/520 nm and 524/572 nm to determine % displacement of the FAM and HEX biosensors, respectively (Figure 5a). We were encouraged to observe that in both of the solutions containing only a single enantiomer of Tym (0 and 100% L-Tym in Figure 5a), the off-target biosensor showed no detectable signal. This further validates the excellent binding selectivity of the aptamer and the lack of fluorescence cross-talk between the FAM and HEX fluorophores. The resulting calibration curves were each fit to a Langmuir binding isotherm using OriginPro. The K_{sens} values for the D- and L-DNA SS biosensors were calculated to be 442 $\pm$ 28 and 464 $\pm$ 29 μM, respectively. These values are significantly higher than the K_{sens} of 160 μM reported for the Peyrin fluorescence polarization biosensor, likely due to the higher ionic strength of the binding buffer used in our experiments. However, given our proposed application of organic reaction monitoring, where typical substrate concentrations are in the high millimolar range, the higher K_{sens} values for our biosensors were not anticipated to be problematic.

To test the accuracy of our calibration curve fitting, we used the resulting Langmuir equation to independently calculate the % L for each Tym mixture. Figure 5b compares the calculated vs actual values of % L-Tym. The deviation between calculated and actual values of % L-Tym ranged from 0.1 to 2.7%, with an average deviation of 0.7%. The error bars on each measurement

DOI: 10.1021/jacs.5b00923
J. Am. Chem. Soc. 2015, 137, 4198−4206

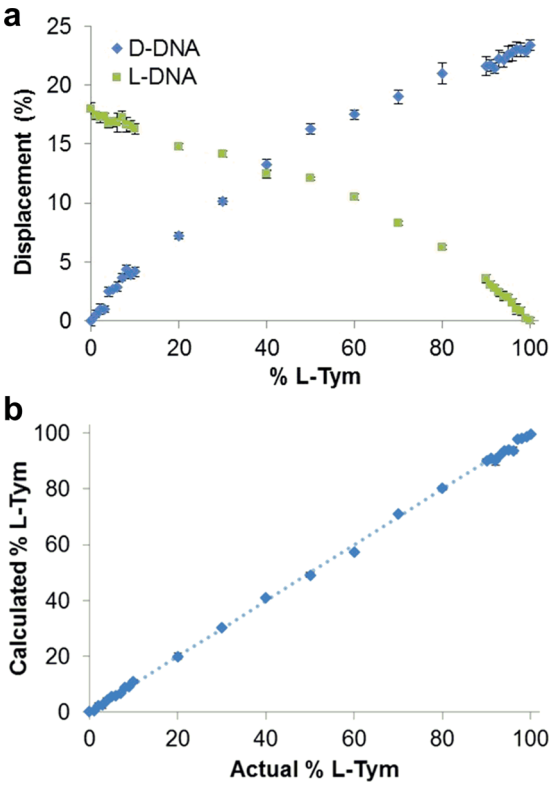

Figure 5. (a) Enantiopurity analysis of samples having varying ratios of L/D-Tym. All samples had a total Tym concentration of 500 μM. (b) Comparison of calculated vs actual % L-Tym. See Supporting Information Figure S4 for expanded views of high-enantiopurity regions.

are calculated from the standard deviation of 3 independent fluorescence experiments, and range from 0.2 to 1.6% with an average error of 0.7%. Together, these data establish a high level of accuracy and reproducibility for our enantiopurity analysis method.

Analysis of Reaction Conditions and Progress. To validate the utility of our enantiopurity analysis method, we chose to apply it to optimization and monitoring of the synthesis of Tym from Tyr-OEt. The importance of reaction optimization for this particular transformation became apparent during our initial experiments using the Tym biosensors. We had set out to synthesize D-Tym using a literature protocol, but observed anomalous results when our "D-Tym" was tested with the SS biosensors. Analysis of our small molecule product using chiral chromatography revealed that a significant degree of racemization had occurred using the reaction conditions reported in the literature (stirring in NH_4OH for 48 h at 4 °C).[42] We hypothesized that this racemization could be suppressed by reducing reaction time, but this would come with the trade-off of reduced yields, and thus optimization would be of high utility.

One unique benefit of calculating enantiopurity from the absolute concentration of each enantiomer is that it also enables simultaneous monitoring of reaction yield. Moreover, our method requires only that a sample from a reaction mixture be diluted into buffer containing the enantiomeric SS biosensors, incubated to allow for equilibration, and analyzed on a fluorescence plate reader. In our experiments, these manipulations required approximately 25 min, but this time could likely be significantly reduced by shortening the equilibration period. Thus, our method has potential to allow for near real-time monitoring of reaction mixtures.

To demonstrate the utility of our biosensors for monitoring the conversion of D-Tyr-OEt to D-Tym, we reacted D-Tyr-OEt with ammonium hydroxide at four temperatures ranging from 10 to 50 °C. While these temperatures are higher than those in the initially reported literature conditions, we reasoned that these conditions warranted investigation, as it was possible that racemization could be minimized by utilizing shorter reaction times, without negatively impacting yield. For each reaction, 100 μL aliquots were removed at 16 time points over the course of 2 h, diluted to 10 mL with binding buffer containing both SS biosensors, and analyzed using a fluorescence plate reader. The % displacement was calculated for each biosensor, and these values were used to independently solve for the concentration of each enantiomer of Tym using our calibration curves.

A plot of the % yield of each enantiomer as a function or time for each of our four reaction temperatures is shown in Figure 6. These data reveal that while increasing the temperature of the reaction increases the rate of product formation, it also increases the rate of epimerization. However, by reducing the reaction temperature to 10 °C, D-Tym can be generated in modest, though reasonable, yield with no observable epimerization after 2 h.

To validate the accuracy of our enantiopurity measurements, we employed chiral HPLC to analyze all of the samples from the reaction carried out at 50 °C. We initially attempted to identify HPLC conditions that would enable baseline resolution of L- and D-Tym, but despite surveying a large number of solvent systems with multiple chiral columns, we were unable to achieve sufficient resolution. However, we were able to achieve good resolution of L- and D-Tyr. Thus, we first used HPLC to separate all Tym from Tyr-OEt, then hydrolyzed the Tym to Tyr using H-form Dowex for 24 h at 100 °C. Finally, we were able to determine the ratio of L- and D-Tyr using an Astec Chirobiotic T 25 cm × 4.6 mm, 5 μm column. To ensure that no racemization occurred during the hydrolysis, we tested this protocol using a mixture L/D-Tym containing 10% L-enantiomer, and measured 9.98% L-Tyr in the final HPLC. The data in Supporting Information Table S4 compare the % L-Tym for the reaction samples as measured by HPLC and using the biosensors, and show an average difference of 1.5% L-Tym, thus validating the accuracy of our reaction monitoring experiments. We highlight that analysis of all of the samples in our study required approximately 1 min of scanning on a plate reader when using our fluorescent biosensors, but would have required approximately 17 h using chiral HPLC, even without the additional hydrolysis and manipulations required specifically for Tym. Thus, this initial reaction monitoring study demonstrates that we can rapidly generate data regarding both yield and enantiopurity for multiple reaction conditions, and that these data can be used to identify optimized conditions for a synthetic transformation in significantly less time than would be required using HPLC.

Enantiopurity Analysis Using SS Biosensors Having Moderate Enantioselectivity. The extremely high enantioselectivity of the Tym SS biosensor enables quantification of individual enantiomers of the target with negligible off-target signal. However, not all aptamers possess such high enantioselectivity, and thus we sought to develop a mathematical model that would enable the measurement of enantiopurity using SS biosensors that have only moderate

DOI: 10.1021/jacs.5b00923
J. Am. Chem. Soc. 2015, 137, 4198−4206

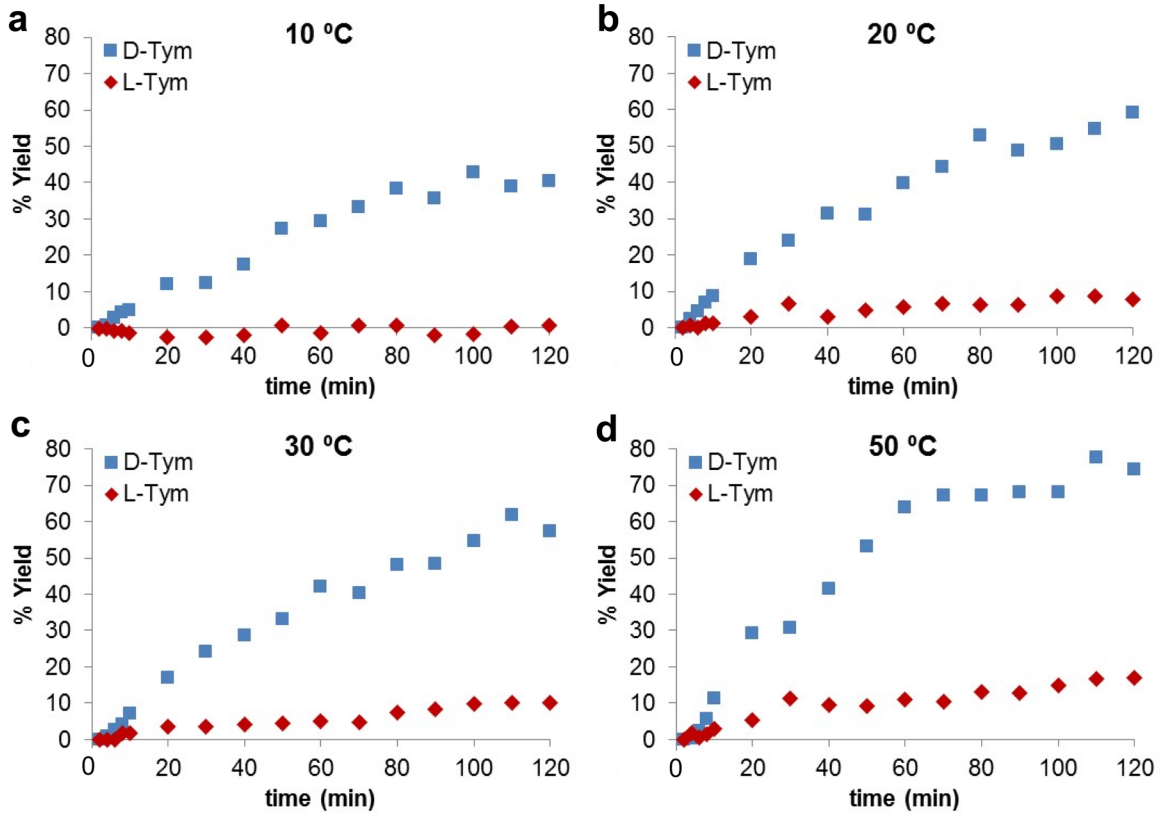

Figure 6. Monitoring the yield of D- and L-Tym during reaction of D-Tyr-OEt with ammonium hydroxide at (a) 10 °C, (b) 20 °C, (c) 30 °C, and (d) 50 °C.

enantioselectivity. Figure 7 shows a calculated representation of the signal that would be observed for enantiomeric SS

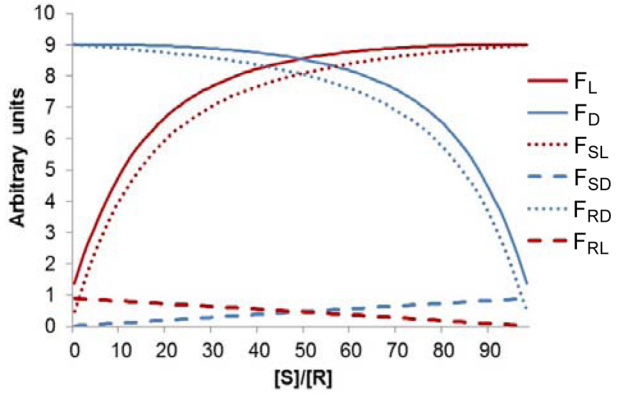

Figure 7. Modeling of fluorescence signal arising from a combination of on-target and off-target binding interactions.

biosensors that bind to a target with 100:1 enantioselectivity. In this graph, the dotted lines represent signal arising from each of the biosensors binding to its target enantiomer, and the dashed lines represent signal arising from the off-target enantiomer. The solid line is the sum of these two signals and represents the total relative fluorescence intensity that would be observed for each of the biosensors (F_D and F_L). The values of F_D and F_L can be used in eq 2 to solve for small molecule enantiopurity (see Supporting Information Figure S5 for full derivation).

$$\frac{[S_i]}{[R_i]} = \frac{\frac{K_4[A^L_{tot}]}{[A^L_{tot}]-xF_L} - \frac{K_2[A^D_{tot}]}{[A^D_{tot}]-yF_D} + K_2 - K_4 + K_1K_4(xF_L) - K_2K_3(xF_L)}{\frac{K_1[A^D_{tot}]}{[A^D_{tot}]-yF_D} - \frac{K_3[A^L_{tot}]}{[A^L_{tot}]-xF_L} + K_3 - K_1 + K_1K_4(yF_D) - K_2K_3(yF_D)} \quad (2)$$

As shown in Figure 8, K_1 and K_2 are the on-target and off-target K_{sens} values, respectively, for the L-DNA biosensor, and K_4 and K_3 are the on-target and off-target K_{sens} values, respectively, for the D-DNA biosensor (specific pairing of the D- and L-DNA biosensors with *S*- and *R*-enantiomers of target was arbitrarily chosen for this model). These values can be obtained empirically by measuring the fluorescence response of each biosensor with varying concentrations of each ligand, then fitting these data to the Langmuir equation. A_{tot} is the total aptamer biosensor concentration. With this equation, the ratio of enantiomers in a mixture can be determined even if a significant (ca. 1%) amount of off-target binding is observed. The primary limitation to this alternative calculation method is that it can only provide a ratio of the two enantiomers, and not their total concentration. However, this information would still be of high value for many reaction optimization applications.

CONCLUSIONS

In summary, we describe here a novel method for the rapid and high-throughput analysis of both small-molecule concentration and enantiopurity. This method relies on the ability of SS nucleic acid biosensors to transduce the presence of a small-molecule target into a dose-dependent fluorescence output, and the ability of enantiomeric SS biosensors to simultaneously quantify both enantiomers of the target molecule. Using our enantiomeric biosensors, we demonstrate the ability to measure the % L-enantiomer in a genuine reaction mixture with an

DOI: 10.1021/jacs.5b00923
J. Am. Chem. Soc. 2015, 137, 4198−4206

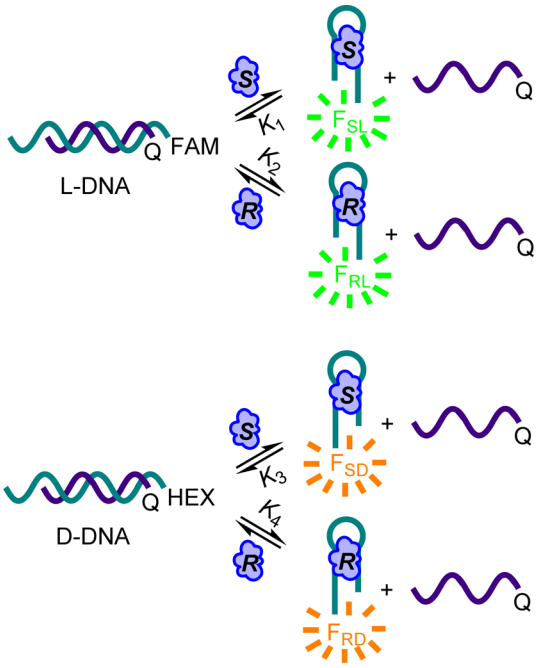

Figure 8. Equilibria involved in on-target and off-target interactions. Specific pairing of the D- and L-DNA biosensors with *S*- and *R*-enantiomers of target was arbitrarily chosen for this model.

average error of 1.5% relative to values determined by HPLC analysis. Additionally, we demonstrate the utility of our method by applying it toward optimization of reaction conditions for the synthesis of D-Tym. Finally, we have generated a mathematical model to demonstrate that enantiopurity analysis is also feasible using aptamer biosensors that possess only moderate enantioselectivity.

Our initial demonstration of this enantiopurity analysis method required significant optimization of the SS biosensor concentration and stoichiometry, as well as identification of the ideal range of target concentrations. However, with the knowledge gained from these experiments, these optimizations could be rapidly performed on a new aptamer system, enabling use of our method to analyze the enantiopurity of a wide range of potential small-molecule targets. Fluorescence-based measurement techniques such as the one described here have potential to enable orders-of-magnitude higher throughput relative to the standard HPLC analysis methods. Thus, we envision that enantiomeric aptamer-based sensors will prove to be a powerful tool for the high-throughput analysis of reaction outcomes, enabling rapid optimization of reaction conditions for the synthesis of specific high-value chemicals.

■ ASSOCIATED CONTENT

Supporting Information

Results from fluorophore orthogonality test, biosensor optimization, HPLC validation, derivation of eq 2, and tabular data for graphs that appear in the manuscript. This material is available free of charge via the Internet at http://pubs.acs.org.

■ AUTHOR INFORMATION

Corresponding Author

*heemstra@chem.utah.edu

Notes

The authors declare no competing financial interest.

■ ACKNOWLEDGMENTS

This work was supported by the National Science Foundation (CHE 1308364 to J.M.H.) and the Army Research Office (59482CH to J.M.H.).

■ REFERENCES

(1) Ariens, E. J. *Eur. J. Clin. Pharmacol.* **1984**, *26*, 663−668.
(2) Jacobsen, E. N.; Pfaltz., A.; Yamamoto, H. *Comprehensive Asymmetric Catalysis*; Springer: New York, 2004.
(3) Reetz, M. T. *Angew. Chem., Int. Ed.* **2011**, *50*, 138−174.
(4) Reetz, M. T. *Adv. Catal.* **2006**, *49*, 1−69.
(5) Jaeger, K. *Curr. Opin. Chem. Biol.* **2000**, *4*, 68−73.
(6) Reetz, M. T.; Zonta, A.; Schimossek, K.; Jaeger, K.-E.; Liebeton, K. *Angew. Chem., Int. Ed. Engl.* **1997**, *36*, 2830−2832.
(7) Knowles, W. S.; Sabacky, M. J. *Chem. Commun.* **1968**, 1445.
(8) McNally, A.; Prier, C. K.; MacMillan, D. W. *Science* **2011**, *334*, 1114−1117.
(9) Szewczyk, J. W.; Zuckerman, R. L.; Bergman, R. G.; Ellman, J. A. *Angew. Chem., Int. Ed.* **2001**, *40*, 216−219.
(10) Finn, M. G. *Chirality* **2002**, *14*, 534−540.
(11) Reetz, M. T.; Wilensek, S.; Zha, D.; Jaeger, K.-E. *Angew. Chem., Int. Ed.* **2001**, *40*, 3589.
(12) Sajonz, P.; Schafer, W.; Gong, X.; Shultz, S.; Rosner, T.; Welch, C. J. *J. Chromatogr. A* **2007**, *1145*, 149−154.
(13) Subramanian, G. *Chiral Separation Techniques: A Practical Approach*, 3rd ed.; Wiley-VCH: Weinheim, 2006.
(14) Kang, J.; Wistuba, D.; Schurig, V. *Electrophoresis* **2002**, *23*, 4005−4021.
(15) Gubitz, G.; Schmid, M. G. *Biopharm. Drug Dispos.* **2001**, *22*, 291−336.
(16) Zhu, Z.; Ravelet, C.; Perrier, S.; Guieu, V.; Roy, B.; Perigaud, C.; Peyrin, E. *Anal. Chem.* **2010**, *82*, 4613−4620.
(17) Drake, A. F.; Grould, J. M.; Mason, S. F. *J. Chromatogr. A* **1980**, *202*, 239−245.
(18) Nieto, S.; Lynch, V. M.; Anslyn, E. V.; Kim, H.; Chin, J. *J. Am. Chem. Soc.* **2008**, *130*, 9232−9233.
(19) Jo, H. H.; Lin, C. Y.; Anslyn, E. V. *Acc. Chem. Res.* **2014**, *47*, 2212−2221.
(20) Reetz, M. T.; Hermes, M.; Becker, M. H. *Appl. Microbiol. Biol.* **2001**, *55*, 531−536.
(21) Sawada, M.; Takai, Y.; Yamada, H.; Hirayama, S.; Kaneda, T.; Tanaka, T.; Kamada, K.; Mizooku, T.; Takeuchi, S. *J. Am. Chem. Soc.* **1995**, *117*, 7726−7736.
(22) Schrader, W.; Eipper, A.; Pugh, D. J.; Reetz, M. T. *Can. J. Chem.* **2002**, *80*, 626−632.
(23) Abato, P.; Seto, C. T. *J. Am. Chem. Soc.* **2001**, *123*, 9206−9207.
(24) Synergy Neo Hts Multi-Mode Microplate Reader. http://www.biotek.com/products/microplate_detection/synergy_neo_hts_multimode_microplate_reader.html (accessed Oct 30, 2012).
(25) Shabbir, S. H.; Regan, C. J.; Anslyn, E. V. *Proc. Natl. Acad. Sci. U.S.A.* **2009**, *106*, 10487−10492.
(26) Leung, D.; Kang, S. O.; Anslyn, E. V. *Chem. Soc. Rev.* **2012**, *41*, 448−479.
(27) Pu, L. *Acc. Chem. Res.* **2012**, *45*, 150−163.
(28) Tuerk, C.; Gold, L. *Science* **1990**, *249*, 505−510.
(29) Robertson, D. L.; Joyce, G. F. *Nature* **1990**, *344*, 467−468.
(30) Ellington, A. D.; Szostak, J. W. *Nature* **1990**, *346*, 818−822.
(31) Geiger, A.; Burgstaller, P.; Von der Eltz, H.; Roeder, A.; Famulok, M. *Nucleic Acids Res.* **1996**, *24*, 1029−1036.
(32) Klussmann, S.; Nolte, A.; Bald, R.; Erdmann, V. A.; Furste, J. P. *Nat. Biotechnol.* **1996**, *14*, 1112−1115.
(33) Williams, K. P.; Liu, X. H.; Schumacher, T. N.; Lin, H. Y.; Ausiello, D. A.; Kim, P. S.; Bartel, D. P. *Proc. Natl. Acad. Sci. U.S.A.* **1997**, *94*, 11285−11290.
(34) Challier, L.; Mavre, F.; Moreau, J.; Fave, C.; Schöllhorn, B.; Marchal, D.; Peyrin, E.; Noel, V.; Limoges, B. *Anal. Chem.* **2012**, *84*, 5415−5420.

DOI: 10.1021/jacs.5b00923
J. Am. Chem. Soc. 2015, 137, 4198−4206

(35) Vater, A.; Klussmann, S. *Curr. Opin. Drug Discovery Dev.* **2003**, *6*, 253−261.
(36) Liu, J.; Cao, Z.; Lu, Y. *Chem. Rev.* **2009**, *109*, 1948−1998.
(37) Jhaveri, S. D.; Kirby, R.; Conrad, R.; Maglott, E. J.; Bowser, M.; Kennedy, R. T.; Glick, G.; Ellington, A. D. *J. Am. Chem. Soc.* **2000**, *122*, 2469−2473.
(38) Jhaveri, S.; Rajendran, M.; Ellington, A. D. *Nat. Biotechnol.* **2000**, *18*, 1293−1297.
(39) Zhu, Z.; Schmidt, T.; Mahrous, M.; Guieu, V.; Perrier, S.; Ravelet, C.; Peyrin, E. *Anal. Chim. Acta* **2011**, *707*, 191−196.
(40) Vianini, E.; Palumbo, M.; Gatto, B. *Bioorg. Med. Chem.* **2001**, *9*, 2543−2548.
(41) Nutiu, R.; Li, Y. *J. Am. Chem. Soc.* **2003**, *125*, 4771−4778.
(42) Yi, G.; Yong-xia, Z.; Xin, J.; Xue-zhong, Z.; Yi, W.; Li, X. *Chem. Res. Chin. Univ.* **2010**, *26*, 942−947.

DOI: 10.1021/jacs.5b00923
J. Am. Chem. Soc. 2015, 137, 4198−4206